Resolving the contact voltage dilemma in organic field effect transistors

M. Koehler,[1,*] I. Biaggio,[2] and M. G. E. da Luz[1]
[1]*Departamento de Física, Universidade Federal do Paraná, C.P. 19044, 81531-990 Curitiba-PR, Brazil*
[2]*Department of Physics, Lehigh University, Bethlehem, Pennsylvania 18015, USA*
(Received 2 October 2008; published 30 October 2008)

In spite of the great interest in organic field effect transistors, many of their aspects are still not well understood. In particular, efforts to uncover the origin of the contact resistance and the underlying physics have lead to apparently contradictory results. Here we show that all these features can be understood by a unified description that takes into account thermionic emission with diffusion-limited injection at the source contact and space-charge limited conduction near it. Moreover, the usual field effect transistors behavior at a certain distance from the source and the conduction in the depletion region emerge not as *ad hoc* assumptions but directly from the proposed mechanisms.

DOI: 10.1103/PhysRevB.78.153312 PACS number(s): 72.20.Jv, 72.80.Le, 73.20.−r, 73.40.Cg

Organic field effect transistors (OFETs) are interesting not only for their applications but also as ideal systems for studying mechanisms of injection and transport in organic semiconductors (OSC). However, some basic aspects are still very poorly understood and are not explained in a self-consistent way by traditional theoretical descriptions.

Remarkably, metal/oxide/semiconductor field effect transistor (MOSFET) equations are commonly used to model the electrical properties of organic transistors. But in many instances the current-voltage OFET responses show a nonlinear increase in the source-drain current (I_{ds}) at low source-drain voltage (V_{ds}), with $I_{ds} \sim V_{ds}^{\beta}$ ($1<\beta<2$), thus strongly differing from the MOSFET curves.[1] Such deviations, generically called contact effects, are attributed to a resistance R_s between the organic layer and the metallic electrodes, whose exact origin is unclear.[2] This resistance plays a significant role in the charge transport of bottom-contact OFETs.[1,3–5] As such, it cannot be ignored in any attempt to obtain the field-effect mobility directly from $I_{ds} \times V_{ds}$ curves.[5,6]

Measurements using bottom-gold contacts and poly(3-hexylthiophene) (P3HT) OFETs showed that R_s goes inversely with the charge-carrier mobility in over four decades [in a broad range of temperatures (T) and gate voltages[5]]. At first sight, this seems consistent with thermionic emission allied to a diffusion-limited injection.[7] However, in such a case one also should expect a strong dependence of the injected current on T, which is not observed for P3HT or for other devices that use lower work-function metals compared to gold and different polymers.[8] Those conflicting findings lead to discount thermionic emission in favor of injection by hopping.[8] As such, models based *only* on the hopping injection of carriers from the metallic source electrode to a random distribution of levels localized in the organic material[8] have been introduced to describe R_s. But these models do not reproduce satisfactorily the experimental current-voltage curves and features such as the large potential drops measured by scanning-probe potentiometry near the source/drain contacts[3] since they do not address the transport process beyond the carrier injection from the electrode.

Here we propose a unified theoretical framework to describe the charge transport near the electrodes and along the channel of bottom-contact OFETs, where high resistivity around the contacts and FET conduction naturally emerge as limiting cases. We show how a diffusion-limited thermionic injection mechanism can be reconciliated with the available data if one considers disorder-induced inhomogeneities in the Schottky barrier height. Moreover, the power-law behavior of $I_{ds} \times V_{ds}$ curves at low V_{ds} is a consequence of structural defects at the OSC/gate-insulator interface that can accumulate so many trapped charges near the electrodes that the whole gate voltage becomes screened, with no free charges remaining in the OSC. This insulating region will then be dominated by a one-dimensional space-charge limited conduction (SCLC). It is the combining effects of SCLC in the vicinity of a contact and inhomogeneous thermionic injection that originate the contact resistance R_s and explain many recent results for OFETs, which up to now appeared to be contradictory.

We call as the "source" contact the one from which the carriers are injected. We assume that the Poisson equation is separated as $dE_y/dy = Q_g$ and $dE_x/dx = Q_{ds}$, for Q_g and Q_{ds} the surface charge densities created by the voltage drop between gate and source/drain electrodes and by the source-drain voltages, respectively.[9,10] The direction x (y) is parallel (perpendicular) to the gate interface. For a OSC film totally free of doping, one finds

$$\frac{I_{ds}}{W\mu} = \epsilon\epsilon_0 D\frac{d^2V(x)}{dx^2} + C_i[(V_g - V_T) - V(x)]\frac{dV(x)}{dx}, \quad (1)$$

with ϵ as the OSC dielectric constant, D as the active layer thickness, C_i as the gate-insulator capacitance per area, W as the channel width, $V(x)$ as the potential at position x from the source, and $V_T = Q_t/C$ as a voltage which represents the effect of traps corresponding to a charge density Q_t. μ is the charge mobility (an effective macroscopic parameter, which characterizes the transport in the system). For $\Delta(x) \equiv E_x^2(x) - E_x^2(0)$ with $E_x(0)$ as the x component of the electric field at the source electrode, the integration of Eq. (1) from the source to a point x in the channel (of total length L) yields[10]

$$\frac{I_{ds}}{W\mu}x = \frac{\epsilon\epsilon_0 D}{2}\Delta(x) + C_i\left((V_g - V_T)V(x) - \frac{V^2(x)}{2}\right), \quad (2)$$

which describes OFETs only when the contact effects are not important. For instance, imposing $E_x(0)=0$ and that the gate-

voltage modulation of the active layer conductivity is small, the first term on the right-hand side of Eq. (2) dominates. As such, by integrating Eq. (2), one finds a space-charge limited conduction $I_{ds} \propto V^2$ (Mott-Gurney law).[11] In Eq. (2), V_T represents the effect of a homogeneous trap density near the source. The electrostatic action of the gate pulls the carriers toward the OSC/gate-insulator interface, where they are then trapped, screening the OSC from the gate potential. As we show next, to correctly model the charge transport not only along the high-conductivity channel but also along the high-resistivity region near the contacts, it is necessary to solve Eq. (2) assuming arbitrary $E_x(0)$ and an appropriate mechanism for charge-carrier injection.

Usually, in real bottom-contact devices,[2,12] the OSC/gate-insulator interface presents structural disorder,[13] leading to a high concentration of traps adjacent to the contacts. To take into account such region (of length d_{sc}), we assume that V_T in Eq. (2) is a steplike potential, zero for $d_{sc} < x < L$, and given by the trap density for $x < d_{sc}$. For simplicity, we assume this region to be close to the source, which has been experimentally observed.[3] Obviously, a similar situation near the drain is also possible. But assuming so makes the model more complicated while not appreciably changing the results (what we have checked). Thus, d_{sc} can be faced as an effective length, which encompasses all the regions presenting substantial trap densities to screen the gate voltage. The resulting voltage drop, $V(d_{sc})$, corresponds to the contact voltage V_c measured in many devices.

For charge injection at the source, we consider diffusion-limited thermionic emission,[11,14,15] $i(\varepsilon) = WDqN_v\mu E_x(0) \times \exp[-(\varepsilon - \gamma\sqrt{E_x(0)})/(kT)]$, successfully applied to describe injection in organic devices[15–17] and appropriate for the common low mobility materials in OFETs.[16] N_v is the density of conducting states, $\gamma = 1/\sqrt{4\pi e^{-3}\epsilon}$ is related to the Schottky effect, and ε is the energy barrier height at the source/OSC interface. This assumption [verified experimentally in a hole conducting OSC (Ref. 16)] accounts for the first tunneling event of the thermionic injection (or thermally assisted tunneling) into the localized states in the organic film.[17]

The disorder-induced inhomogeneities must lead to a statistical distribution $\rho(\varepsilon)$ for the barrier height ε. It can result from randomly oriented molecular dipole moments that create fluctuations in the semiconductor energy levels at the metal/OSC interface.[18,19] To include this effect, we write the total current injected from the source as[20] $I_{inj} = \int_{-\infty}^{\infty} i(\varepsilon)\rho(\varepsilon)d\varepsilon$. Now, for $\rho(\varepsilon) = (\sigma\sqrt{2\pi})^{-1}\exp[-(\varepsilon - \phi)^2/(2\sigma^2)]$, we have

$$I_{inj} = WDqN_v\mu E_x(0)\exp[-(\varphi - \gamma\sqrt{E_x(0)})/(kT)]. \quad (3)$$

$\varphi(T) = \phi - \sigma^2/(2kT)$ is an effective barrier to charge injection,[21] which decreases for decreasing T, comprising the contribution of the multitude of random barriers weighted by the thermal energy. For small T, only the lowest barriers play a relevant role in charge injection. As T increases, the higher barriers also start to be important, leading to a T dependent effective barrier height. This effect can explain the apparent discrepancies between the T dependence of the injected current observed in OFETs and that predicted by thermionic emission.[22] In inorganic metal/semiconductor Schottky diodes,[20] a similar relation between φ and T arises as an analytical limit to simulations of the current across the Schottky barrier, a behavior also observed in Au/CdSe diodes.[23]

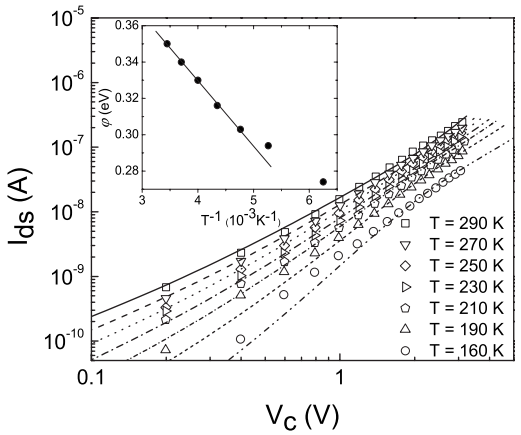

FIG. 1. $I_{ds} \times V_c$ from a set of P3HT/Cr devices with $W = 200$ μm and $V_g = 60$ V. The gate insulator is a SiO_2 layer of 200 nm. The data are from Fig. 7a of Ref. 24 and the continuous curves from the model. Inset: the barrier height as function of T^{-1} with the line a fitting only for $T \geq 210$ K.

We obtain the FET characteristics by varying the value of $E_x(0)$ in Eqs. (2) and (3), finding the corresponding current $I_{ds} = I_{inj}$ from Eq. (3), and integrating Eq. (2) from $x = 0$ to $x = L$, with $E_x(x) = dV(x)/dx$, for the source-drain voltage V_{ds}. Similarly, we obtain the curves $I_{ds} \times V_c$ by following the same procedure but integrating Eq. (2) from $x = 0$ to $x = d_{sc}$ for the contact voltage.

In Fig. 1 we compare our I_{ds} to the experimentally observed dependence on the contact voltage V_c. The data are for gate voltage $V_g = 60$ V, and different T's in an OFET with P3HT as active layer and Cr as source and drain electrodes.[24] We assume $N_v = 10^{26}$ m^{-3}.[25] For simplicity, we always take the modulus of the voltages applied to p-type devices. We fitted the data using adjustable φ, μ, and d_{sc} for each temperature but a common V_T in all cases. At high T's, the model agrees well with the experiments in the whole range of voltages. At low T's and small voltages, thermionic emission diminishes and other mechanisms not included in Eq. (3), such as resonant tunneling,[22] come into play. The data is then higher than the calculated current. At high voltages, thermionic emission is enhanced and becomes dominant [once the factor $\varphi - \gamma\sqrt{E_x(0)}$ in Eq. (3) decreases due to the image charge lowering of the barrier height]. Hence, in Fig. 1 the theoretical $I_{ds} \times V_c$ is in good agreement with the experimental curve in the range of high V_c and any T. From the fitting we obtain $V_T = 50.4$ V and also $\varphi \times T$ (inset of Fig. 1). The straight line for $T \geq 210$ K corresponds to $\varphi = \phi - \sigma^2/(2kT)$ with $\sigma = 0.08$ eV and $\phi = 0.47$ [the latter is corroborated by the fact that the current in P3HT becomes injection limited for barrier heights $\gtrsim 0.5$ eV (Ref. 26)]. Since the P3HT highest occupied molecular-orbital (E_{HOMO}) energy lies between 5.1 and 5.2 eV,[8] and the work function (W) of Cr is about 4.7 eV,[3] a barrier height $E_{HOMO} - W$ within 0.4–0.5 V corroborates our ϕ. Also, the σ from Fig. 1 agrees quite well with the density-of-states widths (80–100 meV)

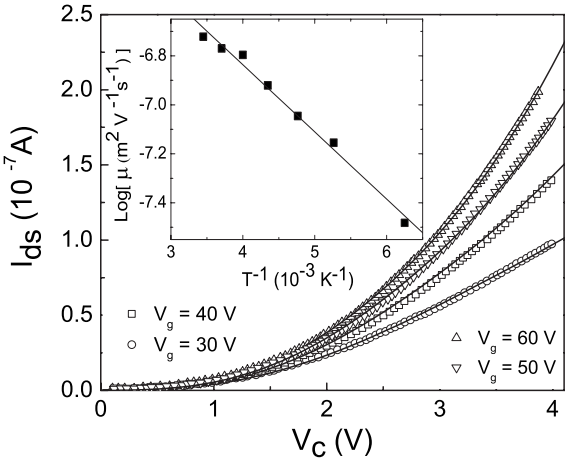

FIG. 2. As in Fig. 1 but for $T=210$ K and different V_g. The data are from Fig. 7b of Ref. 24. Inset: the resulting $\mu(T)$.

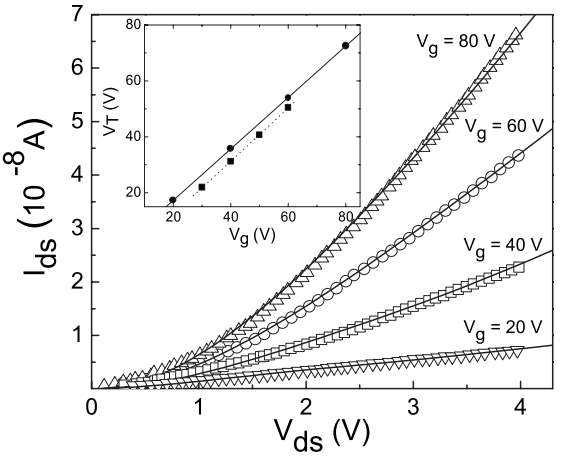

FIG. 3. $I_{ds}\times V_{ds}$ from a P3HT/Au-Cr OFET, with $L=5$ μm, $T=240$ K, and the other features as in Fig. 1. The data are from Fig. 5 of Ref. 24. Inset: the straight lines $V_T\times V_g$ from the fittings of Fig. 2 (circles) and Fig. 3 (squares).

determined in conjugated polymers.[27] Under equilibrium $\sigma^2/(kT)$ is an average energy of carriers in the OSC (Ref. 22) (below the Gaussian density-of-states center). Then, a transition to a regime of charge injection less dependent on T (Ref. 28) is expected for $kT_D \sim \sigma^2/\phi$ (Ref. 18); Here $T_D=160$ K. It explains the deviations for $T<190$ K in Fig. 1. The fit delivers an effective length of the trap region d_{sc} that varies from 70 nm at 160 K to 65 nm at 190 K. From then on, d_{sc} decreases by about 5 nm for each 20 K rise in temperature, understood from the fact that at higher T's thermal excitation starts playing a role in emptying the traps.

In Fig. 2 we again compare our model with the $I_{ds}\times V_c$ characteristics for the same device of Fig. 1 but this time for different gate voltages. The data was taken at a constant $T=210$ K. The only fitting parameters here are d_{sc} and V_T. For φ and μ, we use the values of the $T=210$ K case in Fig. 1. The agreement is very good for all V_g. From the fits we obtain an effective length d_{sc} that decreases for higher gate voltages, as can be expected when more traps are filled in the presence of a larger (gate-induced) density of charge carriers. We find $d_{sc}=100$ nm for $V_g=30$ V, $d_{sc}=75$ nm for $V_g=40$ V, $d_{sc}=65$ nm for $V_g=50$ V, and $d_{sc}=59$ nm for $V_g=60$ V. These values for d_{sc} are very reasonable: an electrostatic modeling of OFETs (Ref. 12) has estimated a large resistance depletion region, about 100 nm from the contacts. Moreover, analysis of the potential profiles in the electrodes vicinity[3] has shown an upper bound of 100 nm for the depletion layer width. We also obtain a V_T that is essentially linear with, also being very close to, V_g. The data is shown in the inset of Fig. 3 (we will return to it below). In general, the change in V_T with the gate voltage can be associated to a stored charge $V_T=Q_t/C_i$.[29] The linear $V_T\times V_g$ behavior suggests that such stored charge originated from injection.

The inset of Fig. 2 shows the mobility from the fit in Fig. 1, well described by $\mu=\mu_0 \exp[-E_a/kT]$, where $E_a=0.057$ eV is the activation energy and $\mu_0=2.05\times10^{-6}$ m^2 V^{-1} s^{-1}. This Arrhenius-like behavior is consistent with simple thermally activated detrapping of the localized states.[28] Our E_a is similar to the values measured for Au-only devices[24] at the same gate voltages.[5]

In Fig. 3 we compare our $I_{ds}\times V_{ds}$ with curves measured for another device,[24] using P3HT as active layer and Cr and Au, respectively, as source and drain electrodes. The data was taken for varying gate voltages at $T=240$ K. We once more use V_T and d_{sc} as fitting parameters for each gate voltage. The values of φ and μ at $T=240$ K are estimated from the Cr-only device in Fig. 1 at $T=230$ K ($\varphi=0.31$ eV and $\mu=1.3\times10^{-7}$ m^2 V^{-1} s^{-1}). A good fit is obtained for all the applied voltages. From the plots we find that also for this Au/Cr device d_{sc} shrinks with increasing V_g: $d_{sc}=120$ nm for $V_g=20$ V, $d_{sc}=85$ nm for $V_g=40$ V, $d_{sc}=80$ nm for $V_g=60$ V, and $d_{sc}=60$ nm for $V_g=80$ V.

For similar V_g, the values of d_{sc} in Fig. 3 (for $T=240$ K) are larger than those in Fig. 2 (for $T=210$ K). This is not an artifact of comparing data at different T's since d_{sc} tends to decrease with rising T. The larger d_{sc} for the Au/Cr device supports the idea[24] that the two-step lithography technique used for the Cr/Au devices produces samples with inferior surface cleanliness and a larger region of high trap density near the source when compared to Cr-only devices. On the other hand, the Cr-only and Cr/Au devices have a similar dependence of V_T on the gate voltage (see inset of Fig. 3), indicating a similar charge stored dynamics. V_T closely tracks V_g, indicating that the effect of traps is indeed almost totally screening the gate voltage. Assuming that the trap states may capture just one positive charge, we can estimate a minimum value for the total surface density of trapping levels[30] required to totally screen the gate voltage: with $V_g=60$ V ($V_g=80$ V) for Cr-only (Cr/Au), we find that the total surface density of trap states is higher than 7.5×10^{16} m^{-2} (9.5×10^{16} m^{-2}).

Finally, we mention that we also have fitted data for polyfluorene F8T2 based OFETs,[1] reproducing the current-voltage curves nicely, even in the saturation region. We have found a linear relation between V_T and V_g, as well.

We have shown that the presence of traps induced by the electrode evaporation process[31] leads to a stored charge near the electrodes that screens the gate voltage. Such traps capture charge carriers from the OSC when they are pushed

toward the interface by V_g. The carrier transport in this region is dominated by space-charge limited conduction, explaining the abrupt voltage drop near the electrodes even in the absence of a barrier height for charge injection at the source. Moreover, carriers are injected by thermionic emission from a random distribution of potential barriers. These two mechanisms are equally important to fully explain the contact voltage observed in OFETs. Their combination results in the peculiar dependences on T and source-drain voltage that have appeared contradictory in view of the previous models.

M.K. and M.G.E.L. acknowledge support from CNPq, Finepe/CT-Infra, CNPq/Universal, and F. Araucária.

*koehler@fisica.ufpr.br

[1] R. A. Street and A. Salleo, Appl. Phys. Lett. **81**, 2887 (2002).
[2] A. Herasimovich, S. Schneinert, and I. Hoerselmann, J. Appl. Phys. **102**, 054509 (2007).
[3] L. Burgi, T. J. Richards, R. H. Friend, and H. Sirringhaus, J. Appl. Phys. **94**, 6129 (2003).
[4] C. B. Blanchet, C. R. Fincher, M. Lebenfeld, and J. A. Roger, Appl. Phys. Lett. **84**, 296 (2004).
[5] B. H. Hamadani and D. Natelson, Appl. Phys. Lett. **84**, 443 (2004).
[6] E. J. Meijer, G. H. Gelinck, E. van Veenendaal, B.-H. Huisman, D. M. Leeuw, and T. M. Klapwijk, Appl. Phys. Lett. **82**, 4576 (2003).
[7] A. Chwang and C. D. Frisbie, J. Phys. Chem. B **104**, 12202 (2000).
[8] B. H. Hamadani and D. Natelson, J. Appl. Phys. **97**, 064508 (2005).
[9] G. T. Wright, Solid-State Electron. **7**, 167 (1964).
[10] M. Koehler and I. Biaggio, Phys. Rev. B **70**, 045314 (2004).
[11] K. C. Kao and W. Hwang, *Current Injection in Solids* (Pergamon, Oxford, 1982).
[12] T. Li, P. P. Ruden, I. H. Campbell, and D. L. Smith, J. Appl. Phys. **93**, 4017 (2003).
[13] Such disorder may be due to either the organic layer deposition along the edges of the vertical contacts or to the evaporation of the metallic contacts. But the relevant point is that both processes lead to trap creation.
[14] P. R. Emtage and J. J. O'Dwyer, Phys. Rev. Lett. **16**, 356 (1966).
[15] J. C. Scott and G. G. Malliaras, Chem. Phys. Lett. **299**, 115 (1999).
[16] Y. Shen, M. W. Klein, D. B. Jacobs, J. Campbell Scott, and G. G. Malliaras, Phys. Rev. Lett. **86**, 3867 (2001).
[17] J. C. Scott, J. Vac. Sci. Technol. A **21**, 521 (2003).
[18] M. A. Baldo and S. R. Forrest, Phys. Rev. B **64**, 085201 (2001).
[19] M. Koehler, M. C. Santos, and M. G. E. da Luz, J. Appl. Phys. **99**, 053702 (2006).
[20] J. H. Werner and H. H. Guettler, J. Appl. Phys. **69**, 1522 (1991); S. Chand and J. Kumar, *ibid.* **82**, 5005 (1997).
[21] E. M. Conwell and M. W. Wu, Appl. Phys. Lett. **70**, 1867 (1997); M. Pope and C. E. Swenberg, *Electronic Processes in Organic Crystals and Polymers*, 2nd ed. (Oxford University Press, Oxford, 1999).
[22] U. Wolf, V. I. Arkhipov, and H. Bassler, Phys. Rev. B **59**, 7507 (1999); V. I. Arkhipov, U. Wolf, and H. Bassler, *ibid.* **59**, 7514 (1999).
[23] C. J. Panchal, M. S. Desai, V. A. Kheraj, K. J. Patel, and N. Padha, Semicond. Sci. Technol. **23**, 015003 (2008).
[24] B. H. Hamadani and D. Natelson, Proc. IEEE **93**, 1306 (2005).
[25] P. W. M. Blom, M. J. M. de Jong, and J. J. M. Vleggaar, Appl. Phys. Lett. **68**, 3308 (1996).
[26] Rashmi, A. K. Kapoor, S. Annapoorni, and V. Kumar, Semicond. Sci. Technol. **23**, 035008 (2008).
[27] A. J. Mozer and N. S. Sariciftci, Chem. Phys. Lett. **389**, 438 (2004).
[28] G. Horowitz, Adv. Funct. Mater. **13**, 53 (2003).
[29] A. V. Ferris-Prabhu, IEEE Trans. Electron Devices **24**, 524 (1977).
[30] W. R. Silveira and J. A. Marohn, Phys. Rev. Lett. **93**, 116104 (2004).
[31] M. Koehler, M. G. E. da Luz, and I. A. Hümmelgen, J. Phys. D **34**, 1947 (2001).